GALILEO GALILEI (GG)

SYSTEM CONCEPT REPORT

DRL/DRD: DEL-20

Written by	***Responsibility***
A. Anselmi	Author
Verified by	
n.a.	Checker
Approved by	
	Product Assurance
	Configuration Control
	Design Engineer
	System Engineering Manager
A. Anselmi	Study Manager
Documentation Manager	

The validations evidence are kept through the documentation management system.

CHANGE RECORDS

ISSUE	DATE	§ CHANGE RECORDS	AUTHOR
draft	31-10-08	Draft circulated before MAR	G. B. Amata
1	17-11-08	First formal issue (unchanged)	
2	13-03-09	IRR issue §1, §2.3, §3.4 to §3.7, §4	
3	08-Jun-09	Issue submitted to PRR	

TABLE OF CONTENTS

LIST OF FIGURES

LIST OF TABLES

1. INTRODUCTION

This document is submitted in partial fulfilment of Work Package 1A-ADA of the GG Phase A2 Study (DRL item DEL-20).

The purpose of the system concept report [SD 2, Annex C] is to describe the principal technical characteristics of alternative system concepts addressed during the study, and the system concept eventually selected as a result of the system trade-offs.

The first issue, prepared for the Mission Assessment Review (11 November 08), provided a review of the previous phases, a reassessment of the intended mission in terms of scientific objectives and expected performance, a new mission analysis and a reassessment of the system concepts, with emphasis on the innovative aspects.

The second issue, prepared for the Intermediate Requirements Review (12 March 2009), provided an updated overview of the status of the design, analysis and performance.

This issue, prepared for the Preliminary Requirements Review (18 June 2009), provides a final overview of the status of the design, analysis and system performance at the end of the Phase A2 study.

2. DOCUMENTS

2.1 Applicable Documents

[AD 1] ASI, “Progetto Galileo Galilei-GG Fase A-2, Capitolato Tecnico”, DC-IPC-2007-082, Rev. B, 10-10-2007 and applicable documents defined therein

2.2 Standards

[SD 1] ECSS-M-00-02A, Space Project Management – Tailoring of Space Standards, 25 April 2000

[SD 2] ECSS-E-ST-10C, Space Engineering - System Engineering General Requirements, 6 March 2009

[SD 3] ECSS-E-10-02A, Space Engineering – Verification

[SD 4] ECSS-Q-00A, Space Product Assurance - Policy and Principles, and related Level 2 standards.

2.3 ASI Reference Documents

[RD 1] GG Phase A Study Report, Nov. 1998, revised Jan. 2000, available at: http://eotvos.dm.unipi.it/nobili/ggweb/phaseA/index.html

[RD 2] Supplement to GG Phase A Study (GG in sun-synchronous Orbit) “Galileo Galilei-GG”: design, requirements, error budget and significance of the ground prototype”, A.M. Nobili et al., Physics Letters A 318 (2003) 172–183, available at: http://eotvos.dm.unipi.it/nobili/documents/generalpapers/GG_PLA2003.pdf

[RD 3] A. Nobili, DEL001: GG Science Requirements, Pisa, September 2008

2.4 GG Phase A2 Study Notes

[RD 4] SD-RP-AI-0625, GG Final Report / Satellite Detailed Architecture Report, Issue 1

[RD 5] SD-RP-AI-0626, GG Phase A2 Study Executive Summary, Issue 1

[RD 6] SD-TN-AI-1163, GG Experiment Concept and Requirements Document, Issue 3

[RD 7] SD-RP-AI-0620, GG System Performance Report, Issue 2

[RD 8] SD-TN-AI-1167, GG Mission Requirements Document, Issue 2

[RD 9] SD-RP-AI-0590, GG System Concept Report (Mission Description Document), Issue 3

[RD 10] SD-SY-AI-0014, GG System Functional Specification and Preliminary System Technical Specification, Issue 1

[RD 11] SD-RP-AI-0631, GG Consolidated Mission Description Document, Issue 1

[RD 12] SD-TN-AI-1168, GG Mission Analysis Report, Issue 2

[RD 13] DTM, GG Structure Design and Analysis Report, Issue 1

[RD 14] SD-RP-AI-0627, GG Thermal Design and Analysis Report, Issue 1

[RD 15] SD-RP-AI-0268, GG System Budgets Report, Issue 1

[RD 16] SD-RP-AI-0621, Technical Report on Drag and Attitude Control, Issue 2

[RD 17] TL25033, Payload Architectures and Trade-Off Report, Issue 3

[RD 18] SD-RP-AI-0629, Technical Report on Simulators, Issue 1

[RD 19] GG.ALT.TN.2003, FEEP Microthruster System Technical Report, Issue 1

[RD 20] TASI-FI-44/09, Cold Gas Micro Thruster System for Galileo Galilei (GG) Spacecraft - Technical Report, Issue 1, May 2009

[RD 21] SD-RP-AI-0630, Spin Sensor Design, Development and Test Report, Issue 1

[RD 22] SD-TN-AI-1169, GG Launcher Identification and Compatibility Analysis Report, Issue 1

[RD 23] ALTEC-AD-001, GG Ground Segment Architecture and Design Report, Issue 1

[RD 24] SD-TN-AI-1218, GG Preliminary Product Tree, Issue 1

[RD 25] SD-PL-AI-0227, GG System Engineering Plan (SEP), Issue 2

[RD 26] TAS-I, Payload Development and Verification Plan, Issue 1

[RD 27] SD-PL-AI-0228, GG System Verification and Validation Plan, Issue 1

[RD 28] SD-TN-AI-1219, Report on Frequency Management Issues, Issue 1

[RD 29] SD-RP-AI-0632, GG Mission Risk Assessment And Mitigation Strategies Report, Issue 1

[RD 30] SD-RP-AI-0633, Report on Mission Costs Estimates, Issue 1

2.5 External Reference Documents

[RD 31] Plasma effects in GG, G. Vannaroni, 19 March 2009

3. SYSTEM CONCEPT REVIEW

3.1 Review of the Scientific Objectives

The review of the experiment objectives, reproduced below, is an abridged version of [RD3]. The significance of the GG experiment remains as high as it was when the GG satellite was addressed in the two ASI studies performed in the past [RD1] [RD2]. The sensitivity objective, too, is unchanged.

The goal of GG is to test the "Equivalence Principle" (EP) to 1 part in 10^{17}, more than 4 orders of magnitude better than today's laboratory experiments. As a consequence of this "Principle" all bodies in the gravitational field of a source mass should fall the same, in vacuum, regardless of their mass and composition. This phenomenon goes under the name of "Universality of Free Fall" (UFF) and is one of the foundations of General Relativity (GR). The need for testing the foundations of GR, hence the Equivalence Principle, is dictated by major current issues such as "dark" matter and "dark" energy, which together account for almost 95% of the Universe and, as the word "dark" indicates, are not understood.

The current state of the art of the ground-based UFF experiments is as follows. Eta = 10^{-12} was achieved with rotating torsion balances at the University of Washington in Seattle, US (recently, an improvement to about 10^{-13} was announced). Lunar Laser Ranging (LLR) has provided a test (for the Earth and the Moon in the gravitational field of the Sun) to 10^{-13}, though it does not allow the sensitivity of the experiment to be tested with test masses of the same composition.

In both cases an intense research activity is ongoing to further improve the sensitivity of the test. However, considerable progress beyond the current level is extremely hard to achieve and unlikely. Only space experiments can aim at testing the Equivalence principle to accuracy orders of magnitude beyond the current standard.

The main reasons for testing the EP in space are:

- As compared to test masses in "free-fall towers", the experiment can last as long as the satellite keeps orbiting the Earth (in the conditions required by the experiment..), certainly much longer than 1 s or less available on ground; in a 1 year measurement the statistical error would decrease by more than a factor 5000!
- As compared to test masses suspended on torsion balances in the lab, the driving signal in space is about 3 orders of magnitude stronger.
- In space, absence of weight allows the test masses to be suspended from the spacecraft much more gently than on ground, where the suspension must withstand the local acceleration of gravity. In space, they are close to free test masses, and therefore they can be proportionally more sensitive to external effects.
- Finally, the orbiting spacecraft enclosing the instrument is an isolated system. Hence the perturbing effects of a laboratory experiment (terrain tilts and seismic noise; motor and bearings noise; nearby mass anomalies not rotating with the instrument) are utterly absent.

The status of the proposed EP space experiments, besides GG, is as follows.

- CNES, with support from ESA, is completing construction of the MICROSCOPE satellite, with the goal of performing an EP test to 10^{-15} (room temperature experiment, about 300 kg total mass at launch). The launch is currently expected to take place in 2011 (the final decision however depends on the status of the micropropulsion, not yet settled; see ESA/SPC(2008)23).
- NASA has been the first space agency to investigate and support an experiment to test the Equivalence Principle in space. That experiment, STEP (Satellite Test of the Equivalence Principle), proposed by Stanford University, is still under investigation. It was studied by ESA too, in collaboration with NASA, in the 1990's. STEP features a cryogenic payload, a large total mass (1 ton at launch) and the goal of reaching 10^{-18}. Today NASA has no firm plans for flying STEP.

GG, so far supported by ASI and INFN, has a conceptually different design with respect to STEP and MICROSCOPE, it does not require cryogenics, has a total mass comparable to that of MICROSCOPE and aims at an EP test to 10^{-17}.

3.2 Review of the Experiment Concept

The GG experiment concept, too, is unchanged from its previous studies. The details of the experiment design, instead, have evolved, as a consequence of the development of the laboratory experiment and the lessons learned in it [RD 2]. See §3.5 below. Importing this experience into the design of the space experiment was an objective of this Phase A2 study.

Eventually, to enable the Implementation Phase to proceed, a set of experiment specifications will have to be frozen. A systematic exercise of laying down the experiment requirements was performed for the first time in this study. The current version of this requirement document is in [RD 6]. This version was agreed with the PI.

An overview of the experiment concept is provided below.

Two test masses of different composition form the GG **differential accelerometer**. The test masses are heavy (10 kg each) concentric, co-axial, hollow cylinders. The two masses are mechanically coupled by attaching them at their top and bottom to two ends of a coupling arm, using soft springs. The coupling arm is made of two concentric tubes similarly attached at their midpoints to a single shaft. This assembly preserves the **overall symmetry** of the apparatus, when the two parts of the arm are taken together.

The masses are mechanically coupled through the balance arm such that they are free to move in the transverse (XY) plane. A differential acceleration acting on the masses gives rise to a displacement of the equilibrium position in the XY plane. The displacement of the test masses is sensed by two sets of capacitance plates located between the test cylinders, one set for each orthogonal direction (X and Y). Each set forms an **AC-bridge** so that a displacement of the masses causes an unbalance of the bridge and is converted into a voltage signal. When the physical system is mechanically well balanced, it is insensitive to `common-mode' accelerations. Moreover, the capacitance bridges are inherently sensitive to differential displacements. Thus, the differential nature of the accelerometer is ensured both by the dynamics of the physical system, and by the displacement transducer.

Testing the EP to 1 part in 10^{17} in the gravitational field of the Earth at 520 km altitude requires detection of a differential acceleration $\mathbf{a_{EP} \approx 8.4 \cdot 10^{-17}\ m/s^2}$. To achieve this sensitivity, the test masses must be very weakly coupled, otherwise the displacement signal resulting from such tiny acceleration is too small to detect. Moreover, the signal (at the orbital frequency) must be up-converted to higher frequency, the higher the better, to reduce 1/f noise.

In the GG accelerometer, the natural period of the differential mode will be designed to be about 545s. At that natural frequency, the EP acceleration signal a_{EP} will produce a displacement $\mathbf{\Delta x_{EP} \approx 0.6\ pm}$ **in the direction of the centre of the Earth**. By spinning the satellite and the accelerometer, with its displacement transducer, around their common symmetry axis, the EP violation displacement signal is **modulated at the spin frequency** of the system relative to the centre of the Earth.

Once the spacecraft has been given the required rate of rotation at the beginning of the mission (1 Hz with respect to the centre of the Earth), no motor or ball bearings are needed inside the satellite. In fact, all parts of the apparatus and the satellite co-rotate around a common symmetry axis. Since the satellite is not constrained to spin slowly, a spin speed which optimizes the stability of the experiment and satellite can be chosen. Due to the very weak coupling between the masses and rapid spin, the GG system is **a rotor in supercritical regime** and supercritical rotors are known to be self-centring even if fabrication and mounting errors give rise to departures from ideal cylindrical symmetry. Moreover, the spacecraft too is passively stabilized by rotation around its symmetry axis and no active attitude control is required for the entire duration of the space mission.

The only disadvantage of spinning at frequencies above the natural oscillation frequencies of the rotor is the onset of **whirl motions**. These occur at the natural frequencies of the system as “orbital” motion of the masses around their equilibrium position. Whirl arises due to energy losses in the suspensions: the smaller the losses, the slower the growth rate of whirl. It must be damped to prevent instability. Provided the **quality factor** Q of the suspensions is at least 20,000 (which laboratory tests have shown to be achievable), whirl growth is so slow that experiment runs can be performed between successive damping cycles, thus avoiding any disturbance from damping forces.

The largest disturbing accelerations experienced by the accelerometer are due to residual air drag and other non-gravitational forces such as sun and Earth radiation pressure. Such inertial accelerations act on the spacecraft and not on test masses suspended inside it, and are, in principle, the same on both the test bodies. Ideally, common mode effects do not produce any differential signal; in reality, they can only be partially rejected. The approach taken in GG calls for surface accelerations to be partially compensated by a **drag free control system**, and partially abated by the accelerometer's own **common-mode rejection**. Drag compensation requires the spacecraft to be equipped with **proportional thrusters** and a control system to force the spacecraft to follow the motion of an undisturbed test mass inside it at (and close to) the frequency of the signal.

Another potential threat is due to temperature effects. **Temperature differences can give rise to differential accelerations** via (a) the "radiometer effect", (b) differential elongation of the coupling arms, (c) differential changes in the stiffness of the suspensions, (d) expansion of the test masses leading to change of their position w.r.t. the capacitance sensors. The temperature requirements, derived in the 1998-2000 study and confirmed in this study, are as follows: 0.2°C/day test mass temperature stability; 1°C axial gradient across the test bodies and the coupling arms. Such performance, which was shown feasible by passive thermal insulation alone, allows 20 days of data taking before rebalancing the test bodies, and at least 15 days before rebalancing the read-out capacitance bridge.

3.3 Launch Vehicle Review

The GG spacecraft shall be compatible with at least one launch vehicle besides Vega. Analysis of the potential options for an alternative, low cost launch vehicle was part of the current study. The status of the launch vehicle review is reported in [RD 22]. The best candidate is the Indian-made Polar Satellite Launch Vehicle (PSLV).

The move to Vega / PSLV eases the satellite accommodation constraints with respect to the 1998 version, tailored for Pegasus (and maintained in the 2002 SSO exercise).

3.4 Mission Analysis

A new mission analysis of the equatorial orbit was undertaken. The current results are in [RD 11]. The study includes, in particular, an updated analysis of the drag acceleration environment in the time period 2013 to 2020, based on the latest available NASA forecast.

A notable innovation, proposed in this study, is to specify the GG mission in terms of a maximum acceleration level, rather than a fixed launch altitude. This allows the experiment and drag free design to be carried out and frozen, independent of the launch date. The launch altitude will be adjusted (within boundaries that do not affect the launcher capability anyway) once the launch epoch is known, in order that the maximum design acceleration is not exceeded.

Figure 3.4-1 shows the results of a parametric study of the maximum drag acceleration, based on the currently determined satellite physical characteristics and the 95% NASA forecast of the solar activity in the solar cycle just started. From 2015 on, the assumed criterion of a maximum acceleration not exceeding 2×10^{-7} m/s² is met at a mean altitude ≥ 700 km. Increasing the launch altitude further could be considered in order to relax the acceleration specification, should this help the equipment (e.g., the microthrusters) meet their performance requirements.

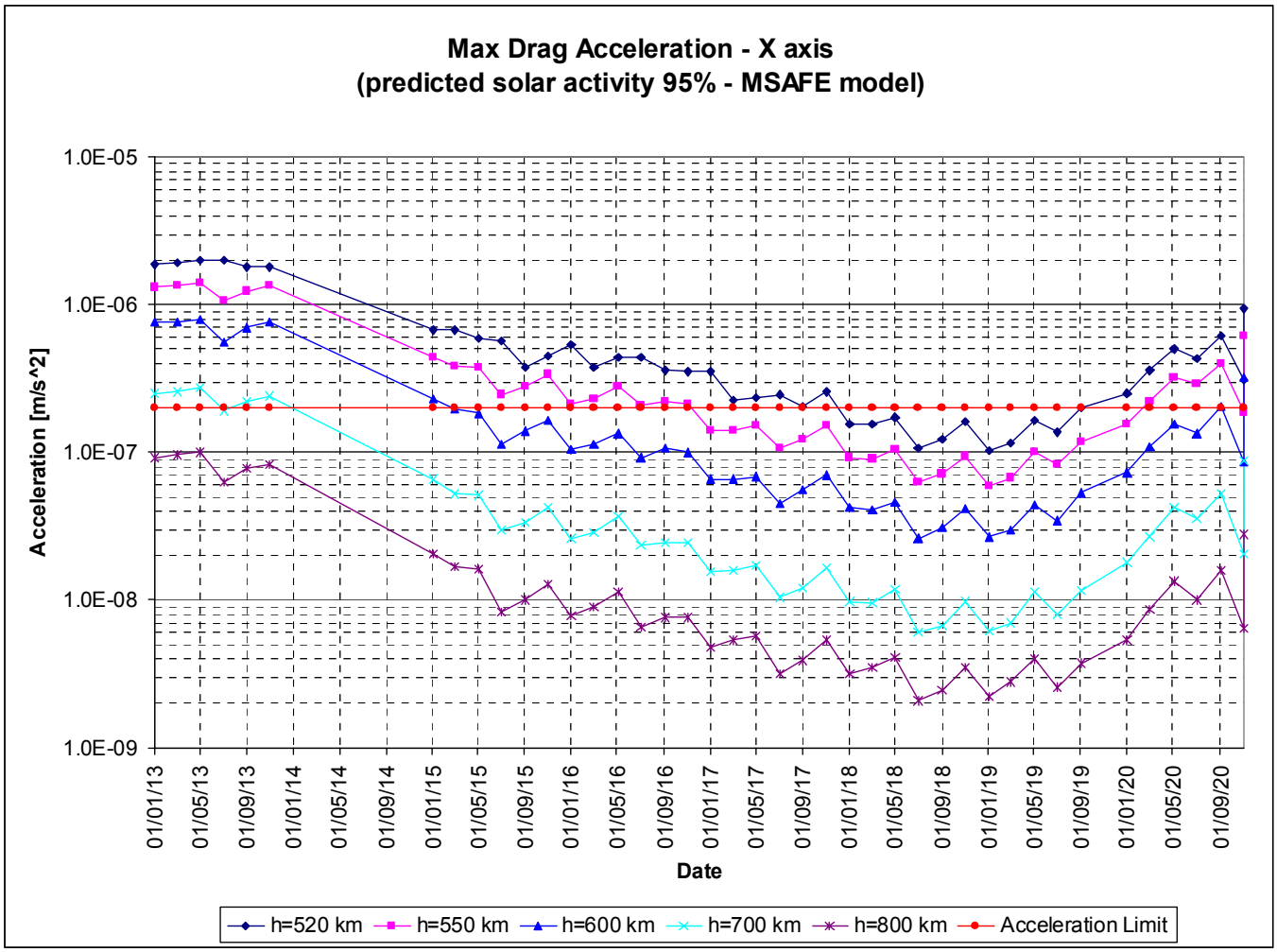

Figure 3.4-1: Parametric analysis of the drag acceleration.

The atmospheric density is taken at the 95% probability level according to the NASA forecast of June 2008. The area-to-mass ratio is 0.0046 m²/kg. A maximum drag acceleration level < 2.0E-7 m/s² first becomes available at mean orbit altitude < 600 km in January 2015 [RD 11].

3.5 Payload Concept

The GG payload is constituted by the PGB (Pico Gravity Box) laboratory, enclosing

- The two cylindrical test masses
- Capacitance plates for “science-level” sensing of test mass relative displacements
- Small capacitance sensors/actuators for sensing relative displacements and damping the whirl motions
- Suspension springs and coupling elements
- Inchworms and piezo-ceramics for fine mechanical balancing and calibration
- Launch-lock mechanisms, associated to all suspended bodies.

The PGB also carries a small mirror, in correspondence of a photo-detector mounted on the inner surface of the spacecraft, for measuring small residual phase lags with respect to the spacecraft.

The payload electronics include:

- The PGB Control and Processing Electronics (CPE), located on the spacecraft platform, managing PGB motion control (whirl sensing, whirl damping and drag-free control) and processing of all signals coming from the test masses (motion control and EP sensing).
- The Experiment Control Electronics (ECE), housed inside the PGB, and communicating with the CPE via an optical link. The ECE locally manages whirl sensing and damper activation, under control by the CPE processor, and readout of the EP chain.

The payload apparatus further includes the necessary electrical harness and connectors and the thermal insulation.

Notable innovations w.r.t. the payload design addressed previously, which have evolved in this Phase A2 study, include the following.

- With respect to the 2003 status [RD 2], the configuration has moved back from the 2-accelerometer (i.e., 4 test masses) design to the simpler single-accelerometer design.
- With respect to the 1998 status [RD 1], the design of the mechanical suspensions has been improved (replacement of flat gimbals and helical springs with U-shaped suspensions; part of the suspension is now rigidly connected to the test masses).
- For the first time, a detailed, hierarchical specification of the experiment requirements was undertaken [RD 6].
- The test mass materials were addressed for technological feasibility as well as scientific performance. The current choice is for a Tungsten alloy for the heavier inner test mass, and high density polyethylene (HDPE) for the lighter outer test mass. The dimensions and inertia properties of the test masses themselves were adapted to reflect the selected materials and the applicable requirements [RD 4].

- Potential plasma induced charging effects on the PGB and their countermeasures were addressed. As an outcome of this analysis [RD 31], it was decided to place a positively polarized grid (repelling the ions) at the PGB inlet (open to allow outgassing).
- Potential magnetic effects on the PGB were assessed, to be damped by wrapping the PGB in a mu-metal shield.
- The configuration of the experiment was modeled in all details, basing on the current configuration of the laboratory experiment (Figure 3.5-1). All properties assumed in the spacecraft models are now firmly based on experimental laboratory evidence.
- The mechanism for passive compensation of the expansion/contraction of the spacecraft, envisaged in the 1998 study, was removed, as it was shown that the effect can be kept small by design, and the rest compensated by the DFACS [RD 16].
- The launch lock mechanisms were designed basing, among others, on the experience gained in similar tasks in the Lisa Pathfinder project.

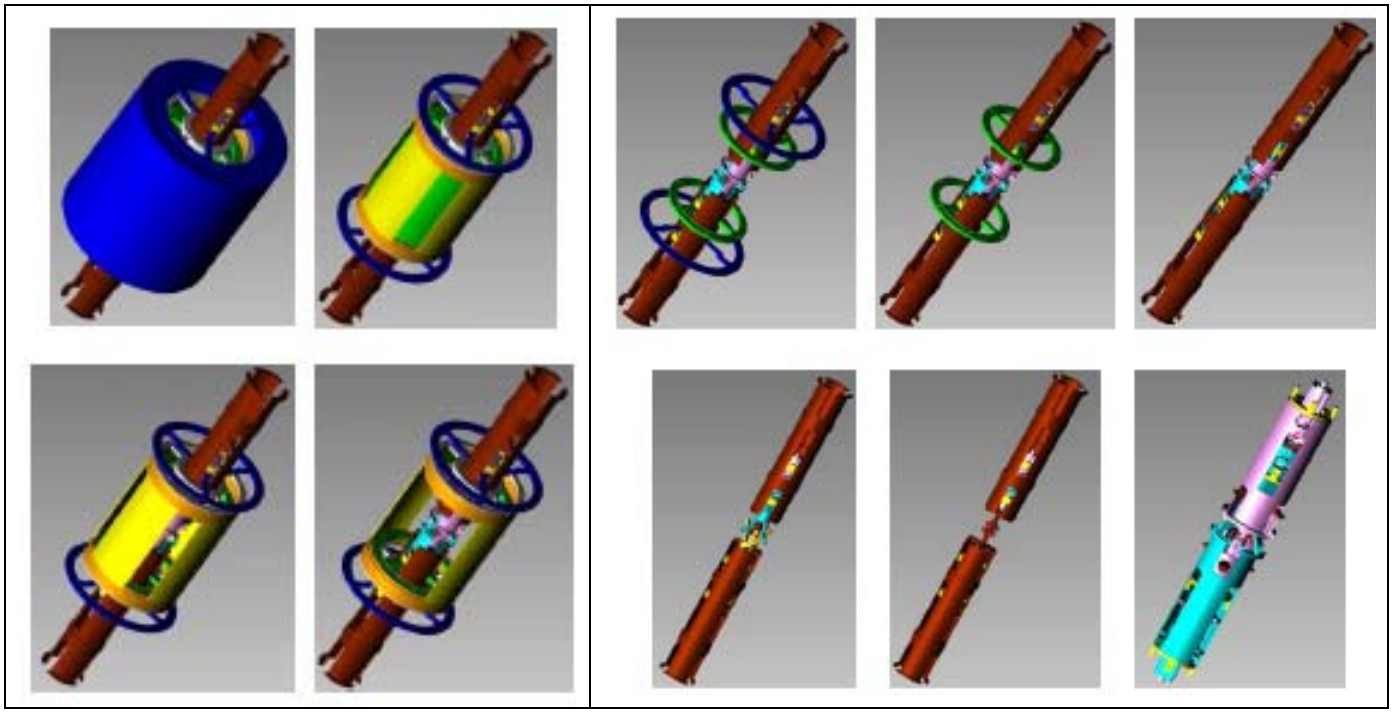

Figure 3.5-1: Details from the engineering drawings of the GG differential accelerometer

The figures disclose the component parts by going further and further from the outside to the inside.

(left) The brown central tube is the PGB shaft. The blue and green cylinders are the test cylinders; the yellow plates are the capacitance bridge plates to measure the relative displacements of the test cylinders. The outer diameter of the blue test cylinders is about 23 cm

(right) In the last picture only the coupling arm remains, and it is clear how it is made symmetric by putting together the two parts (pink and light blue). In the figure before the last, the PGB shaft is well visible, showing its center where the two pieces of the coupling are connected, each one with 3 U shaped laminar suspensions at 120° from each other.

3.6 Spacecraft Concept

3.6.1 Mechanical and Thermal Design

The main drivers of the satellite mechanical configuration are:

- compatibility with Vega launch vehicle and reference fairing envelope;
- outside shape with cylindrical symmetry;
- easy integration of PGB
- spin axis must be a principal axis of inertia;
- low area-to-mass ratio (< 0.005 m²/kg);
- $J_{SPIN} > J_{TRANS}$
- $\beta = (J_{SPIN} - J_{TRANS})/J_{TRANS} \cong 0.2 - 0.3$.

The driving thermal control requirements of GG include:

- test mass mean temperature stability better than 0.1°C/day;
- Axial temperature gradient at the level of the proof masses shall not exceed 1°C/arm length (previous value < 4°C/m);
- Temperature fluctuations in the proof masses shall not exceed 0.2 °C in 1 day;
- Linear temperature drift in the proof masses shall not exceed 0.2°C/day;
- Electronic units (assumed): -20/+50°C operating temperature; -30/+60 °C non operating temperature.

The generic features of the design proposed to meet the requirements are unchanged from the previous studies, and are as follows (Figure 3.6-1).

The requirements of GG do not allow reuse of a standard platform. The proposed solution is an ad-hoc structure with high cylindrical symmetry, supporting the PGB and equipment.

The spacecraft body is about 1.5 m wide and 1.5m high. The experimental apparatus is accommodated in a nested arrangement inside the body. The structure is made up of a central cylinder and an upper and lower truncated cone. The upper cone is removable to allow the integration of the PGB with its suspension springs; the lower cone supports the launcher interface ring. Sensors and electric thrusters are mounted to the central belt. Two S-band antennas, both fixed, are aligned with the spin axis.

The solar array is made of two cylinders separated by a central belt for mounting equipment, including thrusters and sensors; this solution also allows a suitable distribution of thermal covers and radiators to realize an efficient thermal control.

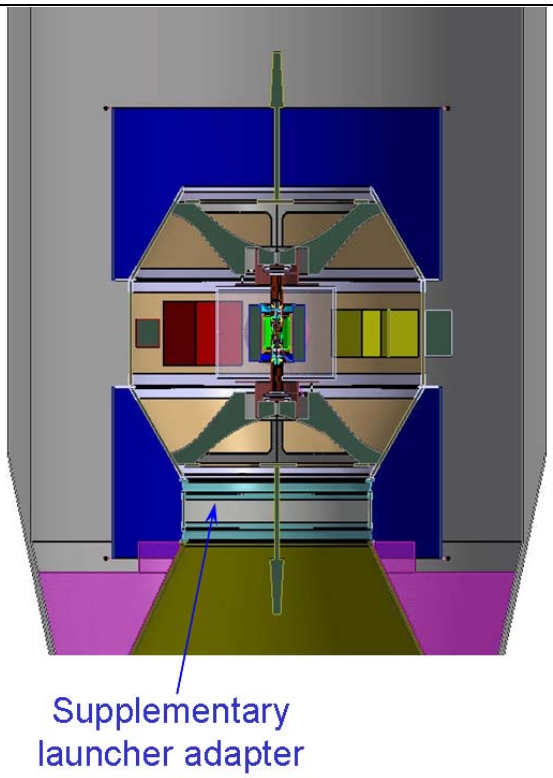

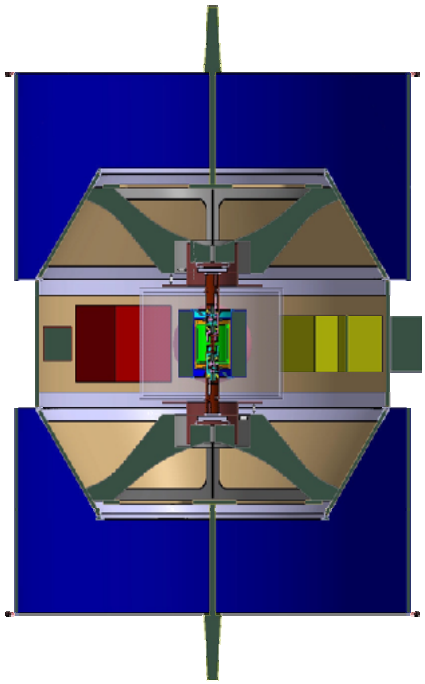

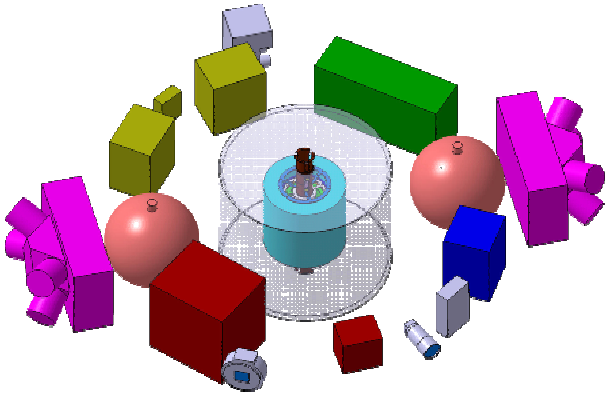

Equipment layout

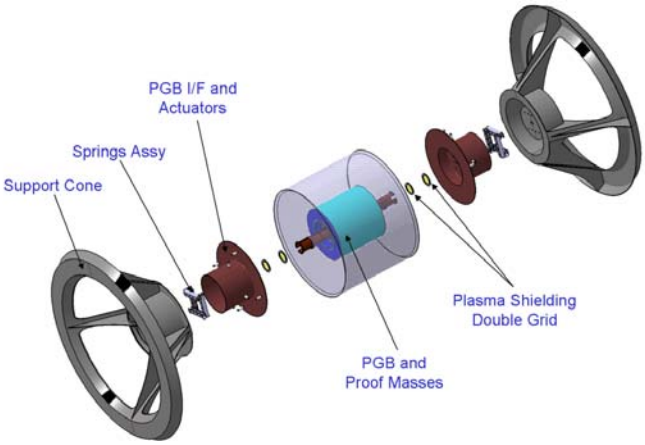

PGB mechanical interface

Figure 3.6-1 : GG satellite configuration

The current implementation of the above-described configuration concept has evolved in this Phase A2 study, as follows.

- To reduce cost, implementation of standard (current-generation) pieces of equipment from the PRIMA platform set was imposed (e.g., transponders, CDMU). These boxes are generally larger than would be possible in an optimized GG-dedicated design. In addition, to avoid costly redesign, all boxes were placed inside the spacecraft body, allowing simpler thermal control. As a consequence, the volume of the spacecraft inflated considerably w.r.t. the previous design exercises (1998 and 2003). This is not considered critical since VEGA allows volume and mass increase well beyond any such requirements of GG.
- The implementation of the FEEP based Microthruster solution benefited considerably from the design data of the current FEEP implementations in Microscope and LISA Pathfinder. A realistic power demand estimate was provided by ALTA, which, together with a detailed design of the solar array, also based on up-to-date parameters, led to an increased area being required for the solar panels. This was accommodated by suitably sizing the panels, while maintaining compliance with the inertia and area-to-mass ratio requirements. This configuration however does not allow further growth (without affecting the inertia and area ratios) and a strict power budget limit must be imposed.
- To make room for the lower solar panel, while remaining compatible with the standard Vega 937 B adapter used for launcher separation, another structural adapter piece had to be introduced.
- A dedicated spacecraft-to-experiment mechanical interface structure was devised.

Layout optimization was performed and inertia and mass balancing was verified compliant with the requirements. A realistic envelope of the FEEP thruster clusters was implemented. Definition of the interface details of such payload elements as capacitance plates, inch-worms and launch-lock mechanisms was much improved.

Very detailed structural and thermal models were implemented (Figure 3.6-2; Figure 3.6-3) and the corresponding analyses were performed [RD 14] [RD 15]. Compliance with the requirements was proven and mass and power resource requirements were updated to reflect these findings.

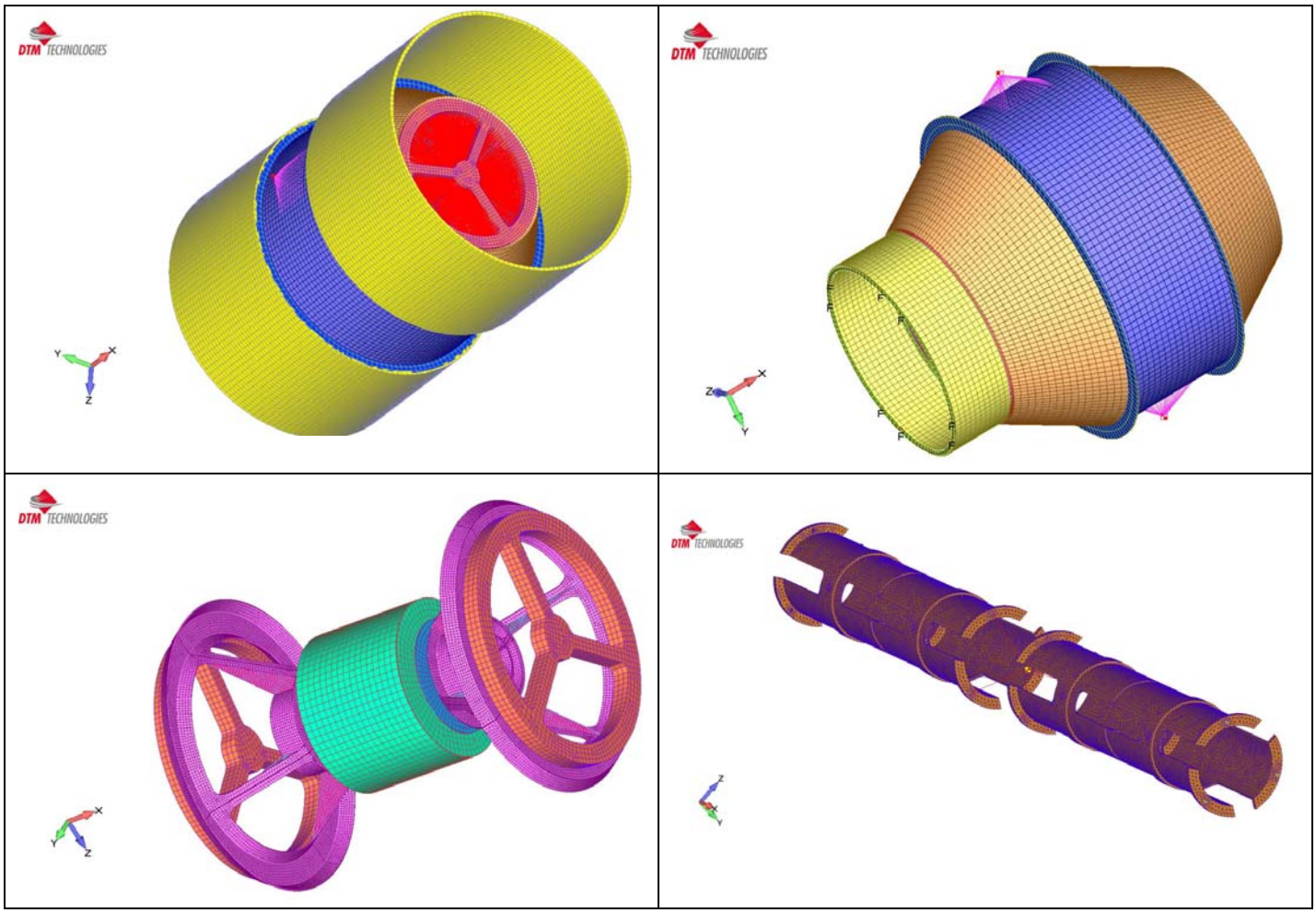

Figure 3.6-2: Views of the structural mathematical model

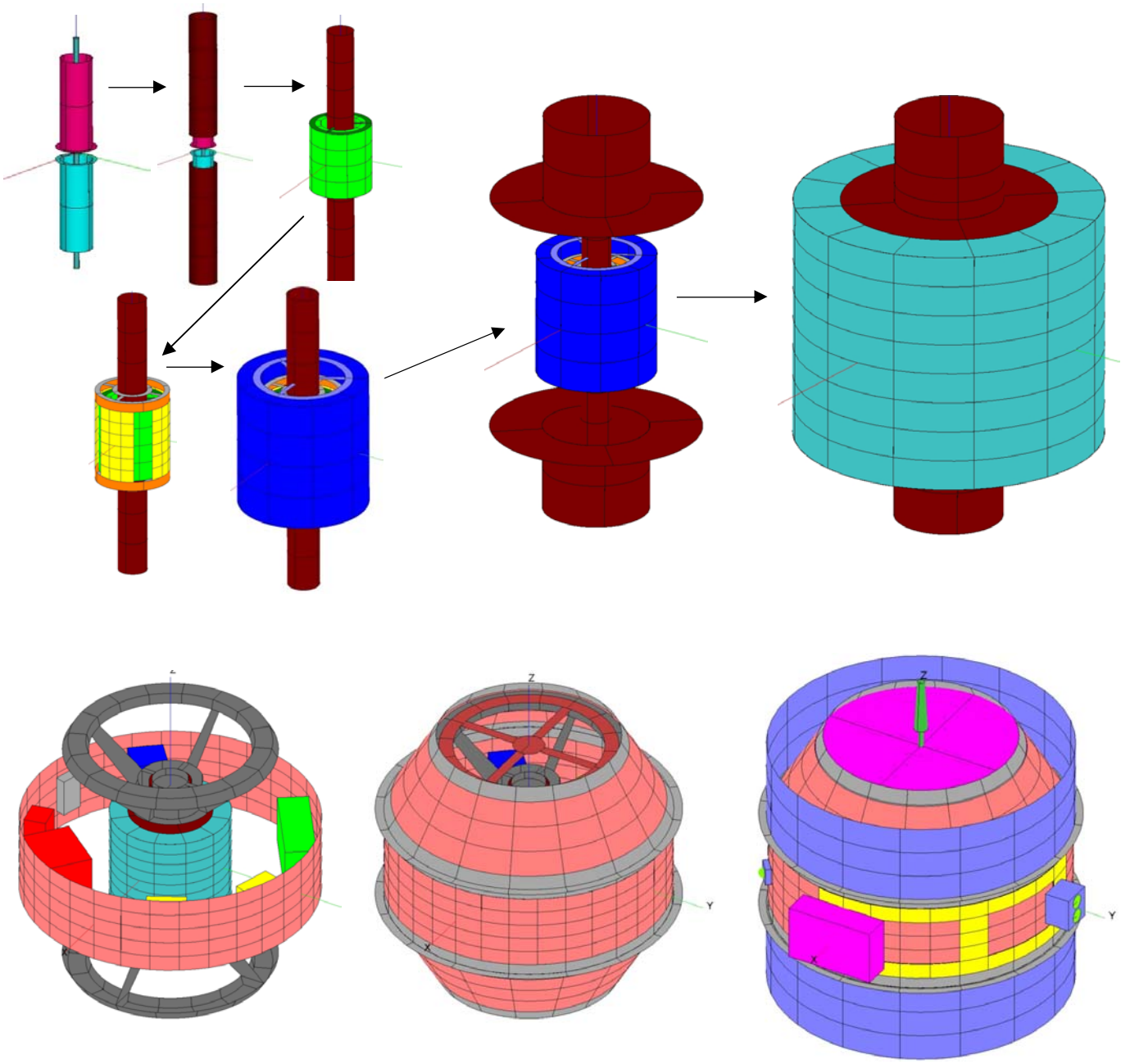

Figure 3.6-3: Geometric thermal mathematical model

3.6.2 Functional and Electrical Design

On-board Data Handling

The GG on-board data handling system (Figure 3.6-4) will be based on a single CDMU, derived from the standard LEONARDO unit, developed via the ASI PRIMA program and based on an ERC32 CPU. A dedicated CPU board, equipped with LEON2FT processor, based on a standard ASIC, is under qualification by TAS-I. If necessary this board could replace the ERC processor board.

The CDMU acts as the central communication node between the Spacecraft and the active Ground Station, distributing or executing commands received from ground and collecting, formatting and transmitting the satellite telemetry.

The CDMU interface with two payload electronics units:

- The PGB Control and Processing Electronics (CPE), located on the spacecraft platform;
- The Experiment Control Electronics (ECE), housed inside the PGB.

The CPE manages PGB motion control (whirl sensing, whirl damping) and processing of all signals coming from the test masses (motion control and EP sensing). Moreover, the CPE performs TC reception from spacecraft and decoding, payload timeline and command execution, science data collection, compression and formatting, TM packetisation and transmission to the spacecraft.

The ECE communicates with the CPE via an optical link. It performs readout of the EP chain and manages locally whirl sensing and damper activation, under control by the CPE processor.

The above-described design concept has evolved in this Phase A2 study, as follows:

- The payload data handing and transmission requirements were clarified and the data rate estimates were consolidated. In particular, it was clarified that all the primary science data will be sampled and sent to Earth at 50 Hz rate;
- The configuration of the payload electronics, in particular the ECE, was developed in accordance with the design of the GGG laboratory experiment.

Radio Frequency Design

An S-Band architecture derived from the PRIMA platform is proposed for the GG TT&C, with minor modifications implemented in the RF distribution network because of the different mission scenario and attitude. The component elements include:

- 2 transponders with low output power (23 dBm, i.e., 200 mW) and diplexer embedded;
- RFDN miscellanea in coaxial technology (2 RF switches and connection cables)
- 2 LGAs with circular polarization (LHCP or RHCP) and hemispherical coverage (gain = -3 dBi at ±95° boresight offset angle).

Assuming Rice-algorithm data compression (compression factor = 2.8), four station contacts per day are enough to download the whole mass memory content.

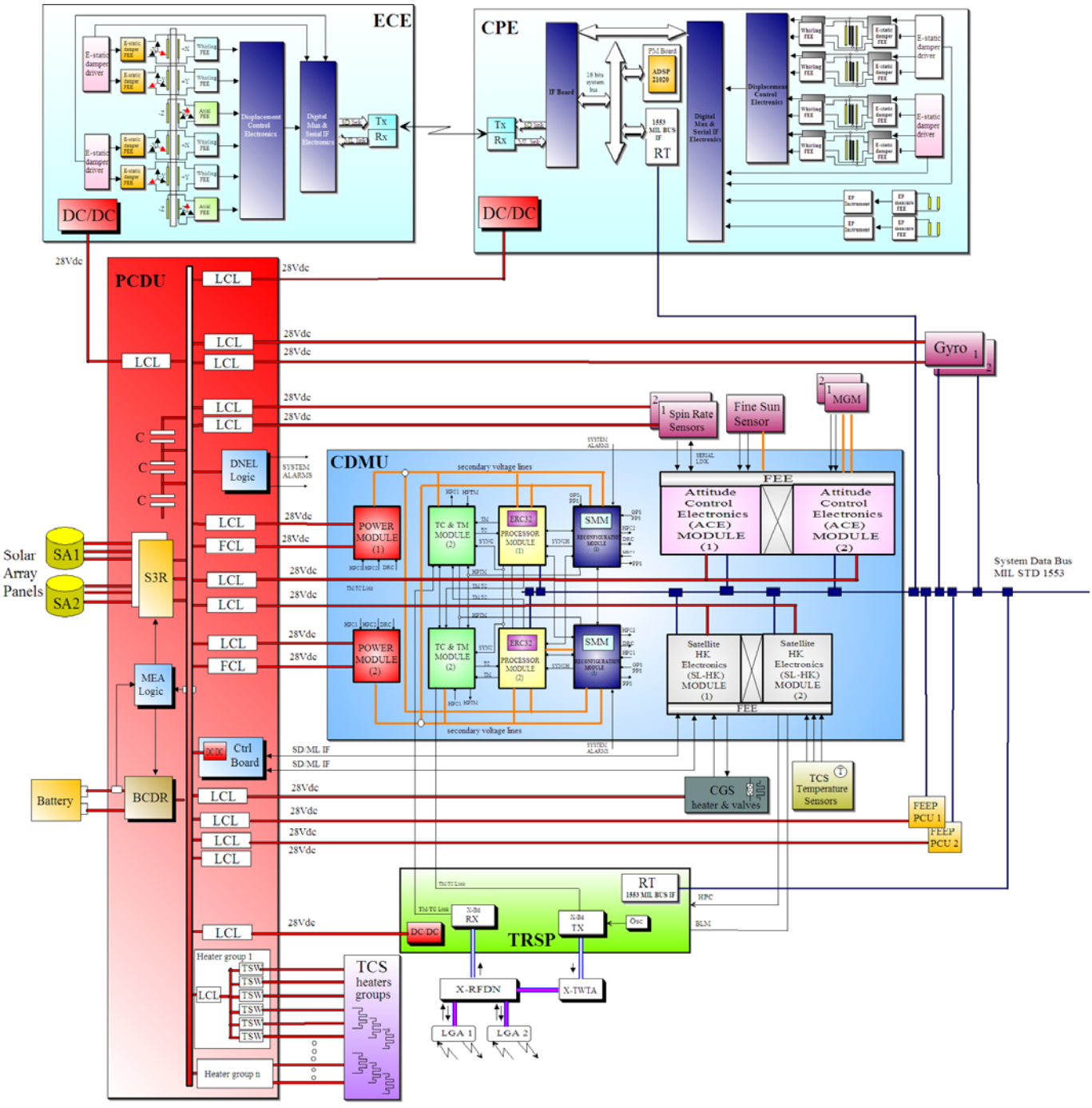

Figure 3.6-4: GG avionic architecture block diagram

Electrical Power

The Electrical Power System (EPS) is required to provide around 500W for both payload and S/C equipment, constantly along the whole mission duration. The EPS is implemented by a dedicated Power Distribution and Control Unit (PCDU), plus power generators and a battery.

The main features of the implemented design are as follows.

- A fully regulated 28V power bus was adopted, compliant with the ESA power standard, under the assumption that the payload electronics only allow operation in a limited range of bus voltage variation. This design also increases the power conversion efficiency in the EPS system and reduces EMC noise.
- For the Solar Array power regulation, both an S3R regulator and an MPPT regulator were considered. An S3R regulator design is preliminarily assumed, considering its simple operation (constant attitude to the sun), the simplicity and robustness of the design and the good flight heritage. By regulating the number of SA sections connected to the bus, the bus is controlled to be at fixed voltage value.
- In series to the S3R regulator, two buck DC/DC converters are implemented, providing the required 28 V power bus voltage conversion and regulation using a Main Error Amplifier (MEA) based on majority voting.
- Taking into account the regulated bus topology, a single BCDR module may be implemented, consisting of two power regulators, a Battery Charge Regulator (BCR) and a Battery Discharge Regulator (BDR).

In addition to consolidation of the architecture described above, the main improvement in this Phase A2 consisted in a more detailed analysis of the solar array implementation requirements, reflected in the currently proposed design [RD 4].

3.6.3 Resources and Budgets

The tables attached provide the status of the resource budgets after the Phase A2 study.

The satellite separated dry mass budget amounts to about 428 kg including 20% system margin. The propellant mass is less than 10 kg in the FEEP micropropulsion option. A two-stage launcher adapter is needed to reach the Vega interface allowing a sufficiently tall solar array. The total launch mass including adapters and all margins is about 518 kg. This is a considerable increase w.r.t. the previous studies, already motivated in §3.6.1.

The power demand of the satellite is about 500W, dominated by the power demand of FEEP. This, too, is a large increase w.r.t. the previous studies, motivated by a 3-fold increase of the estimated FEEP power demand. The solar array as designed now can provide about 10% system margin at BoL w.r.t. the demand. Because of the payload constraints applying to the mass properties, implementing a further increase of the solar array size is not feasible without affecting the whole GG configuration concept.

The data generation rate, shown in Table 3.6-3, is compatible with large margins with the limit telemetry rate of the chosen S-band system and ground station.

Table 3.6-1 : Satellite mass budget

Galileo Galilei					
	Target Spacecraft Mass at Launch			1000,00	kg
	Below Mass Target by:			482,18	kg
	Without Margin	**Margin**		**Total**	**% of Total**
Dry mass contributions		**%**	**kg**	**kg**	
Structure	**104,61 kg**	**18,09**	18,92	**123,53**	23,86
Thermal Control	**8,70 kg**	**20,00**	1,74	**10,44**	2,02
Communications	**9,60 kg**	**10,00**	0,96	**10,56**	2,04
Data Handling	**16,00 kg**	**20,00**	3,20	**19,20**	3,71
AOCS	**5,92 kg**	**13,11**	0,78	**6,69**	1,29
Propulsion	**37,66 kg**	**13,95**	5,26	**42,92**	8,29
Power	**57,68 kg**	**14,82**	8,55	**66,23**	12,79
Harness	**12,50 kg**	**20,00**	2,50	**15,00**	2,90
Payload	**55,34 kg**	**12,77**	7,07	**62,41**	12,05
Total Dry(excl.adapter)	**308,01**			**356,98**	**kg**
System margin (excl.adapter)		**20,00**	**%**	**71,40**	**kg**
Total Dry with margin (excl.adapter)				**428,38**	**kg**
Other contributions					
Wet mass contributions					
Propellant	**4,75 kg**	**100,00**	4,75	**9,50**	1,83
Adapters mass (including sep. mech.), kg	**79,94 kg**	**0,00**	0,00	**79,94**	15,44
Total wet mass (excl.adapter)				**437,88**	**kg**
Launch mass (including adapter)				**517,82**	**kg**

Table 3.6-2 : Satellite power budget

Power Budget (Configuration with 2 FEEP clusters)					Sunlit	Eclipse	
Equipments	No. Of active	Unit Power [W]	Contingency [%]	Power with Contingency [W]	Nominal Power [W]	Nominal Power [W]	LEOP phase [W]
ECE	1	9	20	10.8	10.8	0	0
CPE	1	18	20	21.6	21.6	0	0
Total P/L [W]					**32.4**	**0.0**	**0.0**
CDMU	1	18.0	10	19.8	19.8	19.8	19.8
TRSP1 (Tx + Rx)	1	20.0	3	20.6	20.6	20.6	20.6
TRSP 2 (Tx + Rx)	1	6.5	5	6.8	6.8	6.8	6.8
PCDU	1	25.0	10	27.5	44.5	27.5	27.5
Battery (max charging)	-	-	-	-	180.0	0.0	0.0
TCS (heaters)	1	12.0	20	14.4	14.4	30.0	30.0
Fine Sun sensor	1	1.3	10	1.4	1.4	1.4	0.0
Gyro	0	19.8	10	21.8	0.0	0.0	21.8
Rate Sensor	1	6.0	10	6.6	6.6	6.6	0.0
Magnetometer	3	0.8	10	0.9	2.6	2.6	2.6
FEEP (2 cluster option)	1	133.0	20	159.6	159.6	159.6	0.0
Total Service Module [W]					**456.4**	**275.0**	**129.1**
Total Satellite [W]					**488.8**	**275.0**	**129.1**
PCDU loss [2%]					9.8	5.5	2.6
Harness loss [2%]					10.0	5.6	2.6
GRAND TOTAL w/o system margin [W]					**508.5**	**286.1**	**166.5**

Table 3.6-3 : Satellite data budget

Data description	Variable list	Number of variables	Freq. [Hz]	Record length [bit]	Data rate [kbit/s]
Diff. TMs displacement	0_x, 0_y	2	50	16	1.6
Tme/PGB displacement	0_x, 0_y, 0_z	3	50	16	2.4
Tmi/PGB displacement	0_x, 0_y, 0_z	3	50	16	2.4
PGB/Spacecraft displac.	0_x, 0_y, 0_z	3	50	16	2.4
0_{SPIN}	0_x, 0_y, 0_z	3	50	16	2.4
Reference time	t	1	50	16	0.8
Science data					**12.0**
PGB whirl monitoring	Sensing + actuation	6	1	16	0.096
Tme whirl monitoring	Sensing + actuation	6	1	16	0.096
Tmi whirl monitoring	Sensing + actuation	6	1	16	0.096
ADC monitoring	Number of ADC	9	1	16	0.144
Inchworm monitoring	Number of inchworms	6	1	16	0.096
Piezo monitoring	Number of piezo	6	1	16	0.096
PGB Inner temperature monitoring	Number of temperature sensors	20	0.10	16	0.03
Capacitance bridge monitoring	Number of capacitance bridges	9	0.10	16	0.01
Payload HK					**0.7**
Commands to FEEP	Number of commands	6	1	16	0.096
PGB/Spacecraft phase lag	Number of lag sensors	1	0.10	16	0.0016
Commands to actuators	Number of commands	6	50	16	4.8
Sun sensor	1 (2 in case o redundancy)	2	50	16	1.6
FEEP monitoring	Number of FEEP	6	1	16	0.096
DFACS					**6.6**

Total Data Rate	kbps	**19.3**
Altitude	km	**520**
Period	s	**5702**
Data volume	Mbit/orbit	**110**
	Mbit/day	**1664**

3.6.4 FEEP vs. Cold Gas Micro-propulsion Trade-off

Micro-Newton thrusters are fundamental to achieving the objectives of the EP experiment, and a design driver of the spacecraft configuration. In the past, lack of demonstration of the performance of such microthrusters weighed heavily in the assessment of maturity of all missions proposing to test the EP in space. Considerable progress was made in recent years, and qualification of microthrusters for such programmes as GAIA, Microscope and Lisa Pathfinder is nearing completion.

At the start of this study, two kinds of microthrusters were considered in principle suitable for GG: FEEP (selected for LPF) and Cold Gas Micro Propulsion (CGMP) thrusters (selected for GAIA). Given the past history and the ongoing qualification programmes, for the purposes of the GG Phase A2 study it was decided to keep the decision open until Phase B, unless real showstoppers were identified in one or the other thruster type.

The technical characteristics of the thrusters themselves, compared to the GG DFC requirements, were the subject of a dedicated analysis [RD 16]. The conclusion was that both thrusters are in principle suitable, although not without sacrifice. The time response of the thrusters, in particular, motivated the change of requirement on the spin rate (initially 2 Hz, now 1 Hz). See also §4.2 below.

Moreover, the two kinds of thrusters have very different implications for the spacecraft design:

- FEEP have high power-to-thrust ratio. They drive the solar array size, which cannot grow without limits in the GG satellite. On the other hand, the propellant requirements have negligible impact.
- Cold Gas Micro Propulsion has small power requirements, hence would allow a more compact spacecraft with lower area-to-mass ratio. On the other hand, the propellant requirements are considerable and they, too, are a driver of the spacecraft configuration because of the requirements on symmetry of the mass distribution and the prohibition of moving masses.

The design exercise of this Phase A2 study was based on the FEEP implementation, which is considered the more demanding. The accommodation of CGMP was addressed qualitatively by comparison with the FEEP-driven spacecraft.

3.7 Ground Segment Concept

The preliminary mission and operations requirements of the GG satellite can be summarized as follows [RD 11] [RD 23]:

- Equatorial Orbit at altitude around 600 km
- Utilization of the ASI/Malindi Ground Station
- Additional ground station support to be considered only during early orbit phase and critical spin-up manoeuvre
- Four daily communication passes for TM reception and TC uplink
- Single experiment mission running continuously up to the end of the nominal mission (1 year)
- No scientific quick look is required due to the fact that all science processing is made off-line as bulk data
- No manoeuvres, orbital changes or attitude slews during the scientific mission
- Autonomous scientific operations, executed as time tagged sequences loaded at least one day in advance.

The nominal ground station for mission operations is the ASI GS in Malindi. Additional ground stations may be considered to support the LEOP (for example the ESA Kourou Station that also satisfies the equatorial requirements).

The Ground Communication Network connects the Ground Stations with the Operations Control Centre (OCC), and the OCC with the Science Operations Centre (SOC). It is envisaged that this network can be largely realized using the existing multi-mission ASINET Operational Network.

The Operations Control Centre (OCC) is responsible for the overall execution of the GG mission operations, in terms of mission planning, spacecraft monitoring and control, orbit and attitude determination, P/L monitoring and control. The OCC will route the scientific telemetry to the SOC and will receive the P/L command requests from the SOC to be subsequently processed and uplinked to the satellite. In the current concept, ASI will provide the OCC in the LEOP phase, whereas the scientific mission will be under the control of a dedicated control room at ALTEC.

The Science Operations Centre (SOC) is normally responsible for the scientific data processing and analysis, and for generating the scientific operation sequences to be executed on board. GG is a PI-type mission, where all the data will remain in the possession of the PI, at the University of Pisa, until the first science products have been generated, after which the data will be moved into the public domain. For the GG mission, no real-time involvement of the SOC in the mission operations is required, and the operation sequences are changed very infrequently, if at all, once the experiment has been set up. Therefore, a simple Internet link is envisaged for exchanging the science data between OCC and SOC in an “off-line” mode.

4. CRITICAL TECHNOLOGIES AND SPECIFIC ISSUES OF THE GG MISSION

4.1 Drag Free and Attitude Control System

In this Phase A2, the DFACS advanced very considerably in terms of both design definition and analysis of performance, thanks to in-orbit experience, which was applied to GG by the same design team that successfully designed GOCE, and the development of the advanced GG simulator. The attitude modes, too, were addressed in a thorough way.

The proposed DFACS design is documented in a dedicated report [RD 16]. The document provides:

- a review of the experiment requirements and flow-down of experiment/mission requirements into drag and attitude requirements;
- a proposed attitude and drag-free control architecture;
- a high level design of the operating modes, including both science and non-science modes;
- a detailed design of the control algorithms (drag and whirl) and implementation of them into software mathematical models;
- an analysis of the spin-axis attitude perturbations and design of the attitude control;
- review and identification of the candidate equipment for drag-free and attitude control.

4.2 Micronewton Thrusters

The drag-free and attitude control micro-thrusters must produce finely tuned (in magnitude and frequency) forces, using tiny amounts of propellant in order to minimize perturbations on the test bodies from nearby moving masses. The solution envisaged in the past GG studies was based on Field Emission Electric Propulsion (FEEP) mini-thrusters. These thrusters are very attractive because of the high specific impulse (gas velocity at nozzle exit > 6 km/s) and consequently low propellant mass (a few grams of Caesium suffice for the entire 2-year duration of the mission). Conversely, FEEP has a high power to thrust ratio even if compared with other electric propulsion system. The required thrust is in the same range as needed for the FEEP thrusters under development for the Microscope and Lisa-Pathfinder missions.

The review of the status of the FEEP thrusters was performed with the collaboration of ALTA [RD 19]. Assessment of an alternative option based on the GAIA cold-gas micro-thrusters, produced by TAS-I, was performed too [RD 20]. The comparative analysis [RD 16], performed on the basis of a detailed list of performance and design requirements, found that both thruster types are in principle suitable and mature for GG, although some areas require further investigation. The FEEP implementation was taken as the design reference for this study; however, a final decision is deferred until Phase B, when the outcome of the ongoing Microthruster qualification efforts will become available.

4.3 Spin Rate Sensor

Accurate angular rate measurement with standard sensors (star trackers, sun sensors, earth sensors) becomes critical at large spin rate. Star trackers cannot measure the position of objects moving faster than few tens of deg/s, while the sun/earth sensors are not very accurate. In the previous phases of GG studies, this fact was highlighted as one of the critical aspects of the GG project and it motivated a dedicated breadboard development undertaken as part of this phase A2 study.

The proposed solution for the accurate rate sensor consists of a camera using a Position Sensing Detector (PSD) for measuring the optical power and the coordinates of the light spot focused on the focal plane. A PSD is a four-electrode photodiode in which the photocurrent generated in a given point by a light spot shares between the electrodes proportionally to the position of the spot on the PSD plane. PSD are fast sensors (typical response time = 350 ns) and can provide a very accurate position measurement of the light spot (at the nanometer level, provided to build up a sufficient signal/noise ratio), that translates into an accurate angular measurement through the camera focal length. A small telescope endowed with the sensor detects position of light emitting source from the position of the light spot focused on the PSD. Figure 4.3-1 shows the concept.

A prototype of this novel rate sensor was designed, a performance model was prepared, and the breadboard was manufactured and successfully tested within this Phase A2 [RD 21]. Figures 4.3-2 to 4.3-4 show the breadboard.

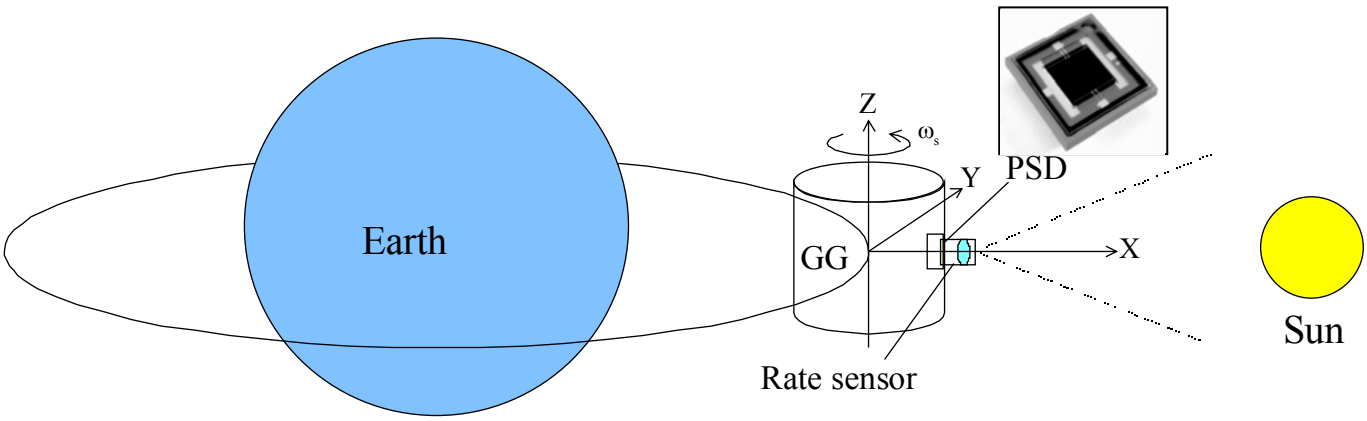

Figure 4.3-1 : Rate sensor arrangement

Figure 4.3-2: Mechanical parts of the spin sensor breadboard.

From right to left: (bottom) spacers and retaining rings; (top) detector box, sensor body, internal optics barrel.

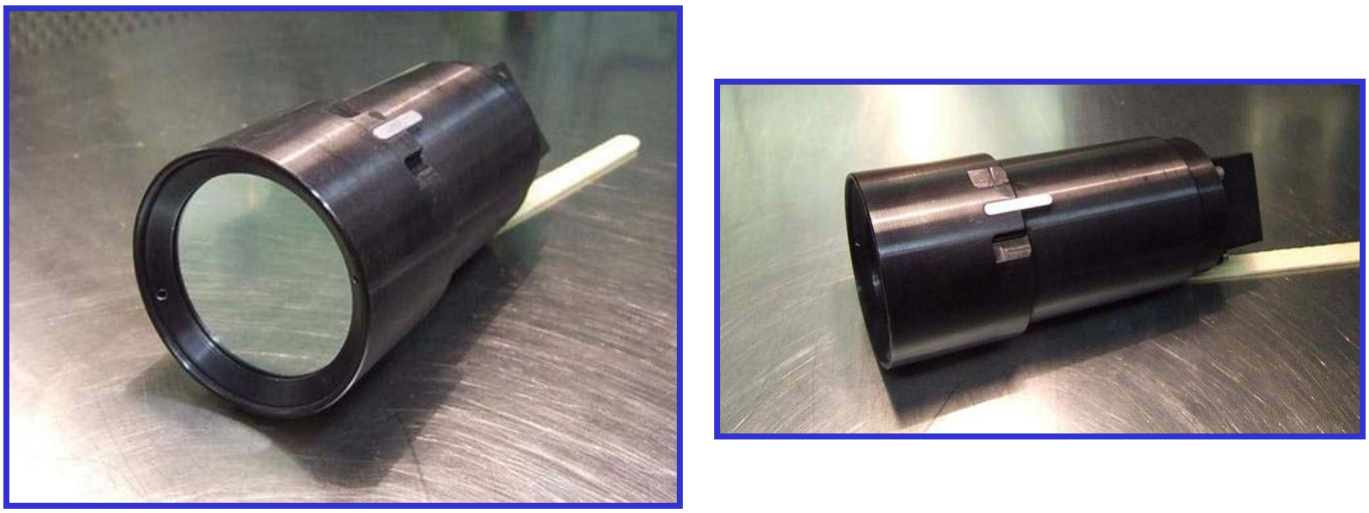

Figure 4.3-3: Fully integrated spin rate sensor

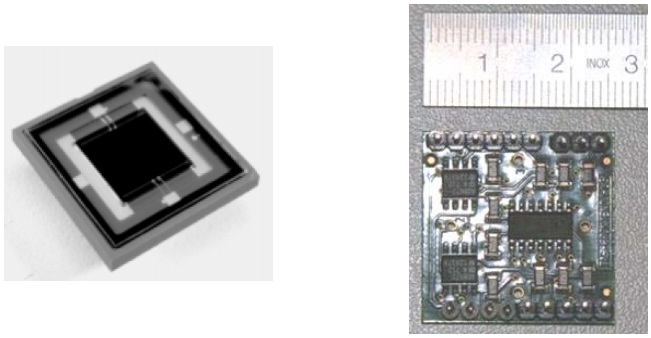

Figure 4.3-4: PSD and front-end electronics

4.4 Software Simulators

A numerical Space Experiment Simulator is a crucial for all space experiments that rely in a fundamental way on zero-g, and therefore cannot be tested on the ground at any level close to the required science performance.

The GG Space Experiment Simulator was initiated, with ASI support, since the first study of the mission, because it was immediately rated as a crucial validating tool. This preliminary simulator allowed the basic physical features of the GG system to be identified and checked; however, it was still too simplified (e.g., it was mostly a 2-dimensional model).

Building up on the expertise acquired with the GOCE Simulator, the GG Space Experiment Simulator could be raised to a very advanced level in the very short time of the GG Phase A2 study. By incorporating in it the physical parameters as experimentally measured in the lab with the Payload Prototype, the accuracy of the simulation was correspondingly enhanced. The combination of (a) flight validation of the orbit and spacecraft environment simulation and (b) lab validation of the experiment parameters, makes the GG simulator an extremely reliable performance validation tool, the like of which was seen in no other similar mission.

Throughout the Phase A2 study, the following steps were performed.

- The latest version of the simulator inherited from the previous studies, was reviewed and updated in order to reflect the current experiment design concept. The simulator architecture is fully modular, which makes it easy to maintain a working version by plugging in the updated modules as they become ready.
- This initial GG system simulator included a model of the spinning satellite constituted by six rigid bodies (spacecraft, PGB, two proof masses and two mechanical suspensions - flat gimbals - connecting the PGB to the test masses). The bodies are connected according to the topology of the true system. A validation campaign on a new hardware platform was carried out.
- A preliminary set of planar (XY plane) simulations was initially carried out to refine the model and verify the performance of the Whirl Control (2-body problem, 6-body problem, with the assumption of no external drag or residual drag).
- Then, a full 3D model of the 6-body system was realised (Figure 4.4-1), providing 6 degrees of freedom to spacecraft, PGB and proof masses and 2 rotational degrees of freedom to the gimballed arm of the suspension (the gimbals allow conical-only movements of the coupling arm of the suspension). The validation was successful.
- The drag-free control law and of the model of the actuators adopted for the drag free compensation were updated according to the latest design.
- Updating of the models of the disturbing forces which can mask/mimic the EP violation signal, and the noise affecting the experiment, were performed
- Implementation of a model of the EP violation signal within the simulator.

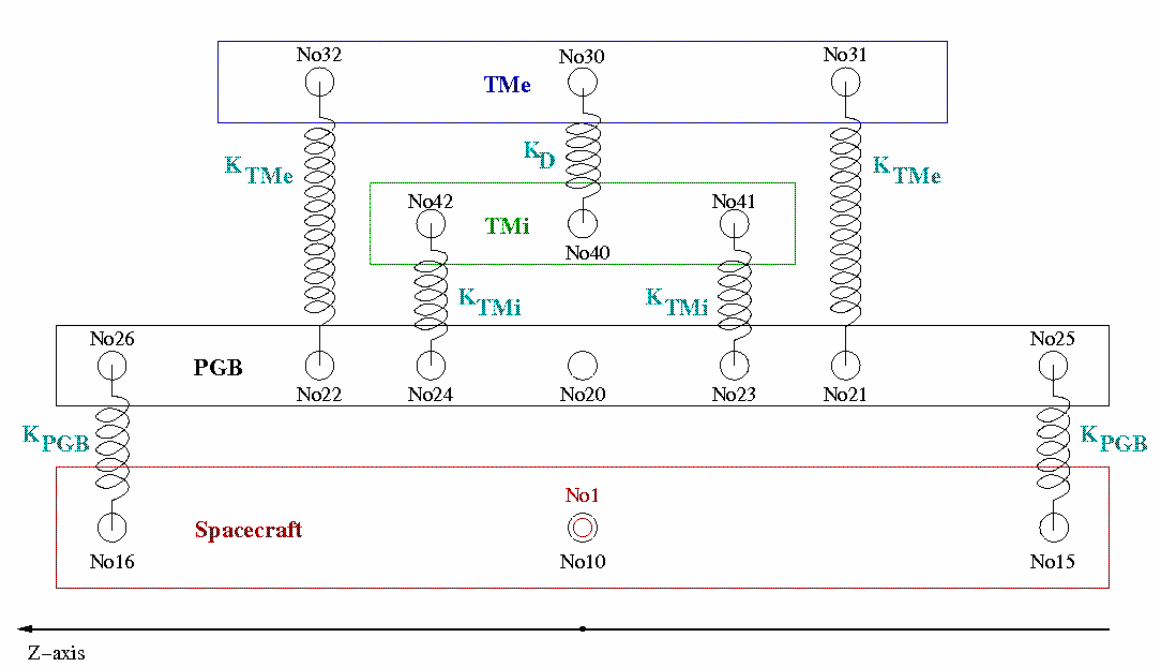

Figure 4.4-1: Schematic model of the GG dynamics system.

Logical scheme of the dynamical model implemented within DCAP software code for finite element simulation of the space experiment. The z axis is the spin/symmetry axis of the system; all elastic connections along z are very stiff; the plane of sensitivity is perpendicular to z. The model encompasses all bodies (spacecraft, PGB and 2 test masses), each one with its 6 degrees of freedom in 3D (3 for translation and 3 for rotation), mass and moments of inertia. All non rigid components of the system (sketched as springs) are implemented with their designed stiffness (in the sensitive plane as well as in the z direction) and mechanical quality factors Q for simulation.

At the end of the above-listed steps, the simulator was ready for its task, i.e., analysis and trade-off of the science performance vs. Drag Free Control and Whirl Control capabilities. The simulator shall produce good indications of the ultimate limit of the science performance depending on the imperfections and noise allocated for the sensors and actuators.

The simulator is capable of excluding one or more control loops (e.g. the Test Mass whirl control, or DFC) from the system in order to analyse and exploit the limit performance for each simplified scenario. This permits to identify each critical point and to establish a hierarchical list of priorities vs. science performance (e.g. the absence of the DFC puts a certain requirements on the Common Mode Rejection Ratio of the mechanical suspension in order to get a given science performance).

In addition, the introduction of the EP violation signal in the simulator provides the capability to test the post processing algorithms that will provide the measurement of the Eötvös parameter.

The documentation of the simulator architecture and the results of the science performance simulation are in [RD 18]. The simulator was also used for the prediction of the ultimate performance of the experiment, documented in [RD 7].

5. ACRONYMS AND ABBREVIATIONS

ASI	Agenzia Spaziale Italiana
BCR	Battery Charge Regulator
BDR	Battery Discharge Regulator
BOL	Beginning Of Life
CDMU	Control and Data Management Unit
CGMP	Cold Gas Micro Propulsion
CNES	Centre National d'Etudes Spatiales
CPE	Control and Processing Electronics
CPU	Central Processing Unit
DFACS	Drag Free and Attitude Control System
DFC	Drag Free Control
DRL	Document Requirements List
ECE	Experiment Control Electronics
EOL	End Of Life
EP	Equivalence Principle
EPS	Electrical Power Subsystem
ESA	European Space Agency
FEEP	Field Emission Electric Propulsion
GG	Galileo Galilei
GOCE	Gravity field and Ocean Circulation Explorer
GR	General Relativity
HDPE	High Density Polyethylene
INFN	Istituto Nazionale di Fisica Nucleare
LEOP	Launch and Early Orbit Phase
LHCP	Left Handed Circular Polarization
LLR	Lunar Laser Ranging
LPF	LISA Pathfinder
MEA	Main Error Amplifier
MPPT	Maximum Power Point Tracker
NASA	National Aeronautics and Space Administration
OCC	Operations Control Centre
PCDU	Power Control and Distribution Unit
PCB	Pico Gravity Box
PI	Principal Investigator
PSD	Position Sensing Detector
PSLV	Polar Satellite Launch Vehicle
RD	Reference Document
RFDN	Radio Frequency Distribution Network
RHCP	Right Handed Circular Polarization
SEP	System Engineering Plan
SOC	Science Operations Centre
STEP	Satellite Test of the Equivalence Principle
TC	Telecommand
TM	Telemetry
UFF	Universality of Free Fall

END OF DOCUMENT